Citation: Dalaijargal, L., T. Hayashida (2020), Estimation of surface wave dispersion characteristics using ambient noise records in Ulaanbaatar region, Synopsis of IISEE-individual study report.

ESTIMATION OF SURFACE WAVE DISPERSION CHARACTERISTICS USING AMBIENT NOISE RECORDS IN ULAANBAATAR REGION

Lkhagvadorj DALAIJARGAL[1] **Supervisor: Takumi Hayashida**[2]

ABSTRACT

We observed Rayleigh and Love wave dispersion characteristics between 5 s and 20 s using yearly-stacked cross-correlation functions (CCFs) of ambient seismic noise data, from the dense seismic broadband network consisting of 17 stations in the Ulaanbaatar region, Mongolia. The extracted empirical Green's functions of Rayleigh and Love waves between 136 pairs of stations showed substantially large signal-to-noise ratios (> 17) in the target periodic range, indicating clear trends of wave propagation up to ~270 km. We removed P-wave contamination, which exists as precursors, from the stacked CCFs using vertical-to-radial (ZR) and radial-to-vertical (RZ) components and succeeded in obtaining dominant Rayleigh-wave signals. The estimated Rayleigh and Love-wave phase velocities using the matched-filter frequency-time analysis showed little variation over the period between 6 s and 10 s, showing small subsurface heterogeneity in the Ulaanbaatar region. The estimated Rayleigh wave phase velocity map for 8 s indicated small (~0.05–0.1 km/s) velocity contrasts between the western and eastern parts, and this suggests the possibility of local-scale seismic velocity heterogeneity in the study area. The resulting velocity maps correspond well with the estimations derived with a sparse seismic array. We also found a feature which could extend our Rayleigh wave phase velocity dispersion to a much longer period, and shorter spacing stations, (which are typically excluded in seismic interferometry) could be included using the SPAC method. The combined use of seismic interferometry and SPAC method will make it possible to conduct a much more precise surface-wave tomographic study in the Ulaanbaatar region.

Keywords: Ambient noise cross-correlation, Ulaanbaatar region, Rayleigh wave, Seismic Interferometry.

1. INTRODUCTION

The Mongolian territory is in the middle of the Central Asian Orogenic Belt (CAOB). The CAOB is situated between the ancient Precambrian Siberian Craton in the north and the Tarim and Sino-Korean Cratons in the south (Badarch et al., 2002). The seismicity of Mongolia is characterized by the effect of the India and Eurasian convergence. Compared to the plate boundary regions, seismicity in Mongolia is relatively low. However, during the last century, large earthquakes (> M8) occurred several times in the Western part of Mongolia, such as Bolnay M8.4 (1905), Gobi-Altay M8.1 (1957), and Tsetserleg M8.0 (1905). The Ulaanbaatar region, the capital city of Mongolia, the seismic velocity structure has not been well investigated due to its low seismicity. Nevertheless, Recent receiver function studies with

[1] Institute of Astronomy and Geophysics, Mongolian Academy of Science (IAG), Ulaanbaatar, Mongolia.
[2] International Institute of Seismology and Earthquake Engineering, Building Research Institute.

teleseismic events have showed the interesting feature that the low velocity zone is investigated at a depth of 10-12 km in study area (e.g. Zorin et al., 2003; Baasanbat et al., 2015). In recent years, the ambient noise cross-correlation technique has become an effective standard tool to construct seismic velocity structures on both local and global scales. Our final goal is to estimate the seismic velocity structure model of the crust and upper mantle using ambient noise records in and around the Ulaanbaatar region. For this purpose, we conduct seismic interferometric analysis using one-year long ambient noise records in the Ulaanbaatar region to extract empirical Rayleigh and Love waves Green's functions.

2. DATA

We analyzed one-year continuous data from 17 broad-band stations in and around Ulaanbaatar region (Figure 1) recorded between January 1, 2018 and January 1, 2019. The 16 broadband stations were equipped with CMG-3ESPC (60 s and 120 s) broadband seismometers (Guralp Inc.) whose sensitivity is 2000 V/m/s. Each sensor is connected to a data logger CMG-DM24S3EAM (Guralp Inc.), and the sampling frequency is set as 50 Hz for all stations. Further to that, we used the station IU.ULN from the Incorporated Research Institutions for Seismology (IRIS), which is equipped with STS-1 (Streckeisen), a very broadband seismometer with a sensitivity of 2358 V/m/s, and recorded with the data logger Quanterra Q330 with sampling frequency 20Hz. All the permanent stations are installed in a concrete vault at a depth of 3 m below the surface. As for the interstation distance, station spacing ranges from 27.92 km to 269.42 km, and the total number of station pairs used in this study is 136.

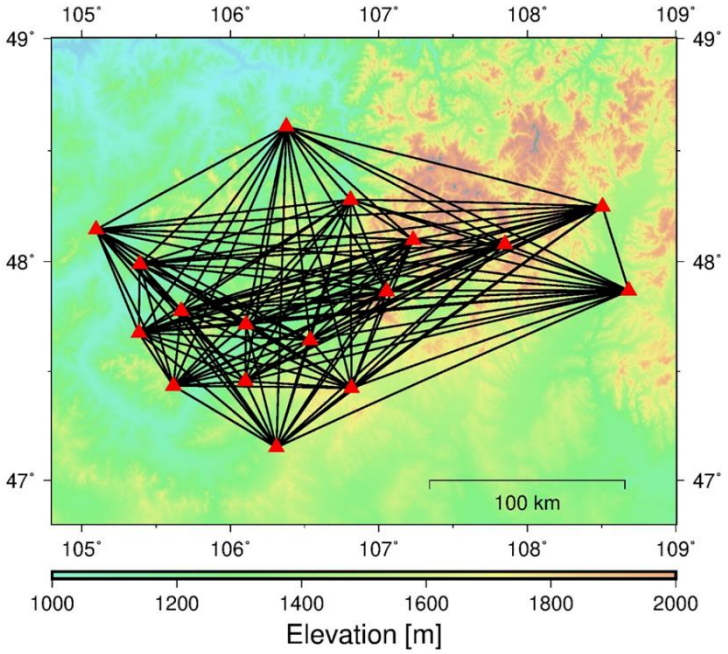

Figure 1. Map showing seismic station distribution (red triangles). The black solid lines indicate interstation paths.

3. METHODOLOGY

3.1. Seismic Interferometry

Recently, surface wave tomography using ambient noise has been widely used to estimate the dispersion of surface waves from regional to global scales. The results from ambient noise tomography agree well with traditional surface wave tomography (e.g. Lin et al., 2008; Pan et at., 2011), and the resulting maps show comparable interpretations in terms of known geological structures such as mountainous ranges and sedimentary basins. In seismology, interferometry based on the ambient noise cross-correlation between two receivers is now a standard and effective tool to illuminate subsurface structures such as crust and upper most mantle of the Earth from the global to regional scale. Seismic interferometry is commonly referred to as the study of interference phenomena between two receivers to obtain structural information of a medium. The main utilization of seismic interferometry is a cross correlation analysis. With a simple mathematical cross-correlation operation, the impulsive response of a medium, known as Green's function, can be extracted assuming one station acts as a source and the other as a receiver. In fact, the noise source distribution is not homogenous. However, under the assumption of the plane wave

propagation and homogenous noise distribution, waves coming from all the direction are destructed except for the two stationary points. Then, the resulting cross-correlogram yields Green's function between the two receivers. The cross-correlation function (CCF) between a pair of two stations can be described as follows:

$$C[x(t), y(t)] = \int_{-\infty}^{\infty} x(\tau) y(\tau + t) \qquad (1)$$

where, x(t) and y(t) are recorded time series at two receivers, and τ is the lag time.

3.2. Green's function extraction

The positive and negative lag signals are observed from the CCF. We then use a symmetric signal to obtain the Green's function. The traditional definition of Green's function is the impulsive response of the point force. So, we estimate approximate empirical Green's function between two receivers $G_{AB}(t)$ from the time-averaged cross correlation Eq. (2).

$$G_{AB}(t) = -\frac{d}{dt}\left[\frac{C_{AB}(t)+C_{BA}(-t)}{2}\right] \; 0 \leq t < \infty \qquad (2)$$

where $C_{AB}(t)$ – positive time lag signal, and $C_{AB}(-t)$ – negative time lag signal. By folding the symmetric parts of the CCF, the signal-to-noise ratio is significantly improved, and the effect of the source distribution's inhomogeneity is greatly reduced. But it alters the signal phase by $\pi/2$, and affects the phase dispersion measurement.

4. DATA PROCESSING

The data processing procedure consisted of three principal phases: (1) single station data preparation, (2) estimation of Green's function, and (3) the measurement of dispersion curves. Here we used an in-house software package developed by T. Hayashida (partially used in Hayashida et al., 2014). The data processing procedure used in this study is mostly based on Bensen et al. (2007). The single station data preparation is intended to eliminate nonpermanent signals (earthquake and instrumental irregularities) from continuous ambient noise records for further cross-correlation analysis. To do that, we first conducted data selections based on two criteria; (a) Daily waveforms must be more than 80 percent (Bensen et al., 2007), and (b) data gaps between each sub traces must be less than 25 s, because we found that the gaps larger than 25 s generate amplitude jumps on the resulting cross-correlation. Data gaps < 25 s were filled with artificial zero amplitudes. Then, all the continuous raw signals were divided into daily sub-traces, and the DC components, liner trend, and the effects of the instruments were removed. A band-pass filter (5–50 s) were then applied to all daily records. After the filtering, daily time-series are down-sampled into 2 Hz to save computation time. After instrumental correction, transient earthquake contaminations are removed by running the absolute-mean normalization method (Bensen et al., 2007). Then after, we conducted the spectral whitening within a window of 0.01 Hz in the frequency domain to flattening the amplitude spectrum at whole frequency range. The main procedure, cross-correlation, is performed in the frequency domain between all components ZZ, ZN, ZE, NZ, NN, NE, EZ, EN, and EE for each station pairs and stacked all daily cross-correlograms. Then, the rotations of horizontal component to radial and transverse directions started just after the stacking to speed up the process using methods of (Lin et al., 2008, Yamanaka et al., 2010). The phase and group velocity measurements were performed using automated procedure frequency-time analysis (FTAN). We used a global crustal structure model (CRUST 1.0; Laske et al., 2013) to estimate the reference dispersion curves of surface-wave phase velocity in the study area. To achieve this, we extracted the 1D crustal model at N47.50º, E106.50º and a program package DISPER80 developed by Prof. Saito (Saito, 1988). For the measurements of group and phase velocities of fundamental Rayleigh and Love modes,

we used a program package aftan1.1 provided by the University of Colorado Boulder (http://ciei.colorado.edu/Products/) for automatic frequency-time analysis (AFTAN) of the CCFs. After the group and phase velocity dispersion measurements, the following selection criteria that was described by Bensen et al. (2007) were used to gather reliable velocity measurements: First, signal-to-noise ratios higher than 17 were selected at the periods of interest. Second, we selected phase and group velocities with interstation distances larger than three wavelengths to satisfy the far-field approximation.

5. RESULTS AND DISCUSSION

The similar symmetric Rayleigh waves with identical arrival times emerged at both positive and negative correlation lags for the Z–Z, R-R, R-Z, and Z-R components. We obtained a reasonable Rayleigh wave without P-wave contamination (Figure 2a) by taking difference between cross-correlation tensors Z-R and R-Z using newly developed method (Takagi et al., 2014). Hereafter, this component is named ZRRZ for further discussion of dispersion measurement. Moreover, clear Love waves were also observed on the transverse-transverse (T-T) component (Figure 2b). In general, the observed Love waves with group velocity ~3.45 km/s showed faster travel time than those of Rayleigh waves observed with group velocity of ~3 km/s. Also, we estimated the signal-to-noise ratio for the yearly stacked cross-correlations of 136 station pairs by taking the ratio between peak amplitude and RMS noise level of trailing noise. In all cases, our estimated spectral SNR satisfy the first acceptance criteria for data selection that the SNR needs to be higher than 17 (Bensen et al., 2007) at the periods of interests between 5 and 20 s.

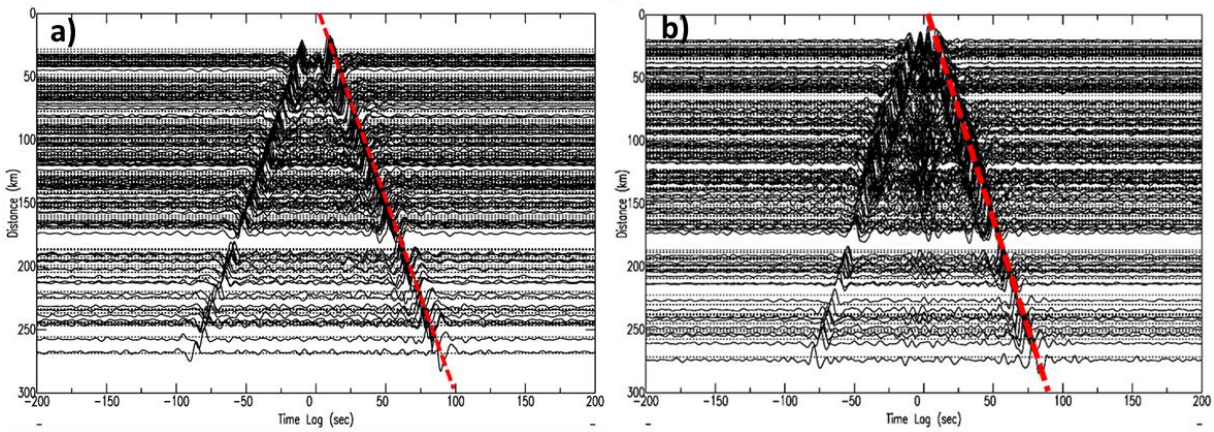

Figure 2. The observed Rayleigh and Love waves from ambient noise cross-correlation between 136 station pairs (a) The Rayleigh wave without body wave contamination on the ZRRZ component ~ 3.0 km/s (b) Love waves on the transverse-transverse (T-T) component ~ 3.45 km/s. The vertical axis shows the interstation distances, and the horizontal axis shows the time lag.

Surprisingly, we observed visible signals on cross terms (T-R, R-T, Z-T, and T-Z), but no clear arrivals were observed. Compared to the diagonal components (Z-Z, T-T, and R-R), these signals were quite weak in most cases. The existence of such signals could be linked to the conversion from Rayleigh-to-Love or Love-to-Rayleigh waves due to the structural heterogeneity, but this is beyond the scope of this study.

We also investigated the feature that there is a $\pi/2$ phase shift between the ZRRZ and Z-Z components. Since such phase difference significantly affects the phase velocity measurement, we incorporated a correction factor in the FTAN analysis. Finally, we measured group and phase velocities using AFTAN on ZRRZ (Rayleigh wave) and TT (Love wave) components for 136 station pairs (Figure 2a and 2c). In this study, the seismic station distribution is typically dense, and station spacing is varied

from 28 to 270 km. Thus, resulting measurements were constrained by interstation distance, and totally 31 station pairs were excluded in data selection.

We observed an interesting feature that a slightly clear velocity contrast emerged at the Rayleigh and Love wave phase velocity map of 8 s. However, both maps presented different characteristics in the western and eastern parts of the study area. As a result of the Rayleigh wave phase velocity map at 8 s, the paths between some station pairs in the eastern area show a relatively smaller value than those of the station pairs in the western part of the study area. In contrast to the Rayleigh wave phase velocity map at 8 s, the Love wave phase velocity map at 8 s presents high velocity in the east and low velocity in the west.

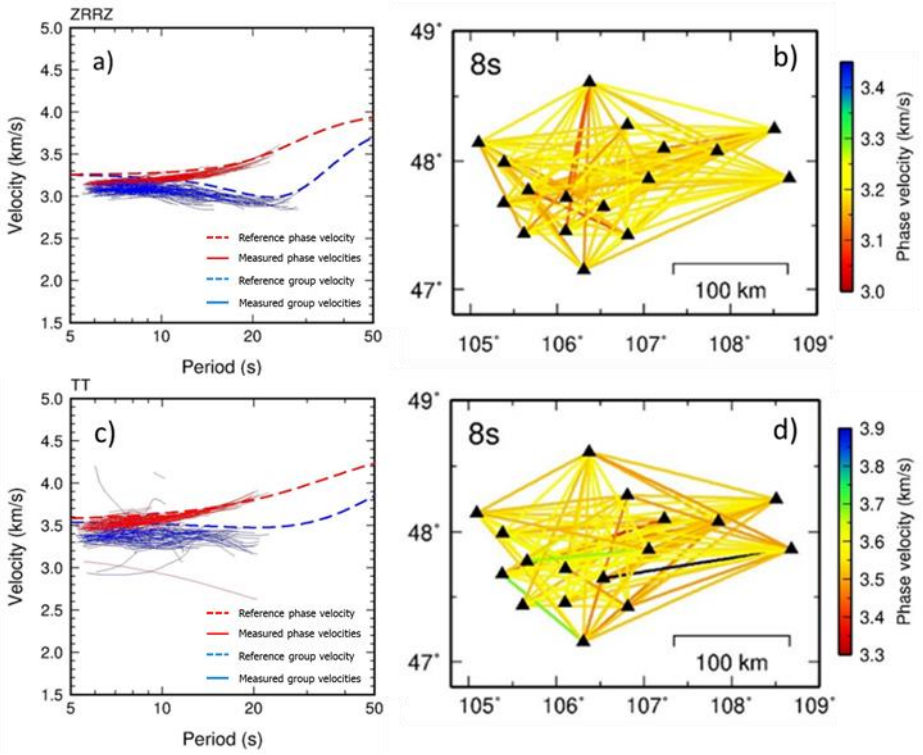

Figure 3. (a) Measured Rayleigh wave dispersions for all station pairs, the reference dispersion curves for both group and phase dispersion curves are shown as blue and red dashed lines, respectively. The red solid lines denote the phase, and blue solid lines denote group dispersion curves. (b) Rayleigh wave phase velocity map of 8s. (c) Love wave dispersion curves, (d) Love wave phase velocity map of 8s.

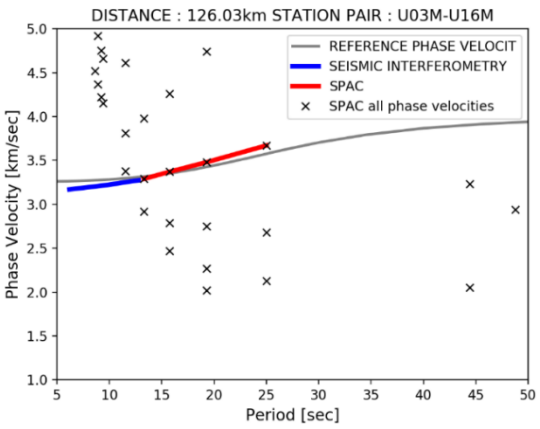

Figure 4. The comparison between the SPAC results and seismic interferometry results.

We investigated the possibility of the estimation of Rayleigh wave phase velocities using the SPAC method (Aki 1957), and compared the estimated results with those from seismic interferometry measurements. Generally, the seismic interferometry uses the main criteria that the distance between two stations must be longer than three wavelengths to satisfy the far-field approximation for selecting the most reliable dispersion measurements. As mentioned before, most of our resulting dispersion measurements are excluded based on these criteria used in seismic interferometry analysis. Alternatively, the SPAC approach can be applied for station separation greater than one wavelength and can also be applied for much longer wavelength measurements (Figure 4).

5. CONCLUSIONS

We observed clear Rayleigh and Love waves from one-year ambient noise cross-correlations using the dense seismic broadband network with 17 seismic stations in the Ulaanbaatar region. The main conclusions are as follows:

1. The estimated SNRs for all station pairs at periods of 5 and 20 s were higher than the required data selection criteria. The ambient noise seems to be weak at periods between about 25 and 50 s.
2. A phase shift was found between the ZRRZ and Z-Z components, and we applied a correction factor to the ZRRZ component in FTAN analysis. After the correction, the resulting Rayleigh wave dispersion curves for both the Z-Z and ZRRZ components were typically similar, and the group velocity dispersion measurements for the ZRRZ component produced relatively stable results than grouped speed dispersion of the Z-Z component. This indicated that the method of separating the Rayleigh wave from the body wave was effective to obtain a stable measurement.
3. Our study was the first case that measured regional Love wave phase and group velocity dispersion measurements in the study area.
4. The Rayleigh wave phase velocity in this study was very similar to the results for previously studied ambient noise in the south-central Mongolian region. Our data will help complement phase velocity maps, obtained with a lack of station coverage in the Ulaanbaatar region.
5. The resulting dispersion measurement from the SPAC analysis presented a significant feature that the dispersion measurement can be extended up to longer periods of around 20 to 30 s. Furthermore, this enables us to perform phase velocity dispersion measurements for longer wavelength even for station pairs with short distances. By combining the results from the seismic interferometry and the SPAC method, we can complement our dispersion measurement with further tomographic analysis.

ACKNOWLEDGEMENTS

This research was conducted during the individual study period of the training course “Seismology, Earthquake Engineering and Tsunami Disaster Mitigation” by the Building Research Institute, JICA. I would like to express my sincere gratitude to my supervisor Dr. Takumi Hayashida for his valuable support and guidance which helped me to complete my research successfully, and to Dr. Tatsuhiko Hara for his guidance and comment during my individual study. I also would like to thank all the other staff members at IISEE/BRI and my international friends in TBIC for their support and encouragement during this training program.

REFERENCES

Aki, K., 1957, Bull. Earthq. Res. Inst., 35, 415-457.

Badarch, G., Cunningham, W.D., and Windley, B.F., 2002, J. Asian Earth Sci., 21, 87-110.

Bensen, G.D., Ritzwoller, M.H., Barmin, M.P., Levshin, A.L ..., 2007, Geophys. J. Int, 169, 1239-1260.

Hayashida, T., Yoshimi, M., and Horikawa, H., 2014, Zishin 2, 66, 127-145.

Laske, G., Masters., G., Ma, Z., and Pasyanos, M., 2013, Geophys, Res. Abstract EGU2013-2658.

Lin, F.C., Moschetti, M.P., and Ritzwoller, M.H., 2008, Geophys. J. Int, 173, 281-298.

Okada, H., 2003, Geophysical Monograph Series No.12, Society of Exploration Geophysicists, Tulsa.

Pan, J.T., Wu Q.-J., Li, Y.-H., Yu, D.-X., Gao, M.-T., Ulziibat, M., and Demberel, S., 2015, Chin. J. Geophys., 58, 436-450.

Saito, M., 1988, Academic Press, ed. by Doornbos, D.J, 293-319.

Takagi, R., Nakahara, H., Kono, T., and Okada, T., 2014, J. Geophys. Res.: Solid Earth, 2005-2018.

Takeo, A, Nishida, K., Isse, T., Kawakatsu, H., Shiobara, H., Sugioka, H. and Kanazawa, T., 2013, J. Geophys. Res., 118, 2878-2892.

Ts, Baasanbat, Shibutani, T., 2015, IISEE/BRI, 1-63.

Yamanaka, H., Chimoto, K., Moroi, T., Ikeura, T., Koketsu, K., Sakaue, M., and Nakai, S., 2010, BUTSURI-TANSA (Geophysical Exploration), 63, 409-425.

Zorin, Y.A., Mordvinova V.V., and Turutanov, E.K., 2002, Tectonophysics, 359, 307-327.